

Article

Structure and Heat Transfer Characteristic Evolution of CaO-SiO₂-CaF₂-Based Solid Mold Flux Film upon Solidification

Xiao Long ^{*}, Wenbo Luo ^{*}, Xiang Li, Shaolei Long, Honggang Ma, Dayang Luo and Congxin Zheng

School of Materials and Energy Engineering, Guizhou Institute of Technology, Guiyang 550025, China

^{*} Correspondence: llx580@sina.com or xiaolong@git.edu.cn (X.L.); 20180902@git.edu.cn (W.L.)

Abstract: In this study, two typical commercially used CaO-SiO₂-CaF₂-based mold fluxes with different basicities were adopted. Solid slag films of the two mold fluxes were obtained by immersing an improved water-cooled copper probe in the molten fluxes for different probe immersion times and molten slag temperatures. The film thickness, closed porosity, and roughness of the film surfaces in contact with the copper probe were measured. The heat flux through the solidified films and the comprehensive thermal conductivity of the films were both calculated. The results indicated that compared with the heat flux through high-basicity films, the heat flux through low-basicity films exhibited high fluctuation due to the evolution of fusion cracks within the glass layer. High-basicity mold fluxes resulted in higher thickness, growth velocity, surface roughness, and devitrification velocity of the films. With the growth and crystallization of the slag films, the comprehensive thermal conductivity of the high-basicity films increased significantly. For the low-basicity films, their comprehensive thermal conductivity first decreased and then increased after the solidification time exceeded 30 s. The comprehensive thermal conductivity of the high- and low-basicity films ranged from 0.63 to 0.91 and 0.62 to 0.81 W/(m·K), respectively. The results provide a novel method for analyzing the potential effect of the structural factors of slag films on heat transfer control and controlling the heat transfer behavior of slag films.



Citation: Long, X.; Luo, W.; Li, X.; Long, S.; Ma, H.; Luo, D.; Zheng, C. Structure and Heat Transfer Characteristic Evolution of CaO-SiO₂-CaF₂-Based Solid Mold Flux Film upon Solidification. *Metals* **2024**, *14*, 1. <https://doi.org/10.3390/met14010001>

Academic Editors: Mariola Saternus and Ladislav Socha

Received: 25 October 2023
Revised: 14 December 2023
Accepted: 14 December 2023
Published: 19 December 2023



Copyright: © 2023 by the authors. Licensee MDPI, Basel, Switzerland. This article is an open access article distributed under the terms and conditions of the Creative Commons Attribution (CC BY) license (<https://creativecommons.org/licenses/by/4.0/>).

Keywords: mold fluxes; solid slag films; structure; heat flux; comprehensive thermal conductivity

1. Introduction

Mold fluxes are vital materials applied in the continuous casting of steels. They are essential for improving the surface and subsurface quality of casting slabs and maintaining smooth casting [1–4]. During steel casting, mold fluxes are continuously added and melted in the molds to form a slag pool on liquid steel. The melted slag then flows into the gap between the initial steel shell and mold wall to form solid and liquid slag films. The solid slag film in contact with the mold wall controls the heat flux from the steel to the mold [5–8]. As one of the essential metallurgical functions of mold fluxes, heat transfer control capability is considered a crucial feature in the evaluation of slags. In particular, during the continuous casting of peritectic grades, mild cooling of the initial steel shell is required; this is especially important for a crack-free surface, because the peritectic reaction and fast cooling can cause significant volume shrinkage on the weak initial steel shell, increasing internal stress [9–13].

As the heat transfer control capability of a solid slag film is directly determined by its structure, the structure of mold flux films, especially upon cooling, has been extensively evaluated. Most existing studies have focused on the crystallization features of solid films [14–18]. Recently, qualitative results related to the effects of typical film structures on heat transfer have been reported [19–21]. However, the structure of a solid film is significantly affected by the cooling conditions. Moreover, several factors can cause slag films acquired in a laboratory to exhibit non-representative structures [22]. Some studies have used improved water-cooled copper probes to obtain solid films with structures

similar to those of films solidified in molds (with the same slag composition). Using this improved technique, the steady-state thermal contact resistance between the solid films and molds and the effective thermal conductivity of the solid films were calculated [23]. However, only the steady state (the film grows to a steady structure with a steady heat flux) can be calculated using this method.

As the initial solidified steel shell is quite weak, the structural and heat transfer control capabilities of initial solid slag films near the meniscus are essential [1–3]. Understanding the evolution (especially at the initial solidification stage) of the structures and thermal conductivity of slag films is a prerequisite for understanding and controlling the metallurgical functions of solid slag films.

To address the limitations of previous studies [22,23], an improved water-cooled copper probe was used in this study to obtain solidified slag films (with structures similar to those of films solidified in molds) and heat flux data through these films. Solidified slag films with different probe immersion times were obtained to analyze the evolution of film structures during solidification. The microstructure of the solid slag films was preserved by intensive cooling from the contacted water-cooled copper wall after the probe withdrew liquid slags. In addition to the structure of the slag films, the heat flux through the films during solidification was calculated using the temperature increase in the cooling water passing through the probe. Based on the structural evolution behavior of the films and corresponding heat flux through the films, the transient-state heat transfer behavior of the slag films during solidification was calculated and discussed. In this study, the typical substructure and thermal conductivity evolution of solidified films were calculated and discussed.

Two typical CaO-SiO₂-CaF₂-based mold fluxes (high and low binary basicities) were selected as the basis for this study. The structure and comprehensive thermal conductivity evolution of the slag films during solidification were determined. Our research results provide a novel method for analyzing the potential effect of structural factors of slag films on heat transfer control and controlling the heat transfer behavior of slag films upon solidification.

2. Experiments

2.1. Mold Flux Selection and Slag Film Solidification

Two commercially used mold fluxes were adopted in this study to reveal the potential causes of the performances of mold fluxes with different basicities. The compositions of the selected conventional CaO-SiO₂-CaF₂-based mold fluxes are presented in Table 1. Two basicities were used in this study. Different fusion agents were added to adjust the physical properties of the slags. Samples for experiments were prepared using analytical-grade reagents CaCO₃, SiO₂, Al₂O₃, CaF₂, Na₂CO₃, LiF, Li₂CO₃, and MgO. To prepare the slag samples for film acquisition, the reagents were loaded into a high-purity graphite crucible and melted in a resistance tube furnace at 1300 °C. The liquid slags were poured on a water-cooled copper plate to obtain quenched glasses.

Table 1. Composition of mold fluxes (wt%).

No.	CaO	SiO ₂	F	Na ₂ O	Al ₂ O ₃	Li ₂ O	MgO	Basicity
1	41	32	10	11	3	-	1	1.28
2	34	40	8	13	2	1.5	1	0.85

(All components were represented as oxides, except for F).

For each film acquisition experiment, 300 g of pre-melted slag lump was loaded into a high-purity graphite crucible with an inner diameter of 60 mm. This crucible was then placed into a vertical tube furnace with Si₂Mo heating elements and heated to experimental temperatures (1300, 1350, and 1400 °C) until the end of the film acquisition experiments. To obtain the solid slag film, a water-cooled copper probe with a width of 20 mm, height of 15 mm, and 6.35 mm in thickness was immersed in the slag bath (immersion depth 13 mm;

flow rate of cooling water 1.7 dm³/min), and the solidified slag film was recovered from the probe after experiments. To investigate the structural evolution behavior of the solid slag film, different probe immersion times (15, 30, 45, 60, and 90 s) were used. Because the basicity of slags significantly affects the growth speed of films, the low-basicity film had a low growth velocity (more time was needed for the film to reach a steady state upon solidification); probe immersion times of 15, 30, 60, and 90 s were applied. For the high-basicity film, probe immersion times of 15 s, 30 s, 45 s, and 60 s were used.

2.2. Measurements and Analysis

The heat flux through the slag film was calculated using the temperature increase in the cooling water upon passing through the probe. Heat flux can be expressed using Equation (1), where Q is the heat flux, MW/m²; W is the flow rate of cooling water, kg/s; $(T_{out} - T_{in})$ is the temperature increase in cooling water, K; A is the area that the probe contacted with slag films, m²; and C_p is the heat capacity of water. More detail on heat flux calculation can be found in references [19–24].

$$Q = \frac{(T_{out} - T_{in})W \cdot C_p}{1000A} \quad (1)$$

Because the heat transfer velocity in solid slag films is significantly lower than that in the copper wall and forced-convection liquid slag, the temperature difference between the copper wall of the probe (contacted with solidified films) and the solidification front of the slag films before reaching a steady state was assumed to be equal to the temperature difference between the cooling water and liquid slag. Thus, a comprehensive thermal conductivity of a film with a given solidification time can be expressed using Equation (2), where Q is the heat flux through films, λ is the comprehensive thermal conductivity of slag films (containing contact thermal resistance between slag film and copper wall), L_{film} is the thickness of obtained slag film, and T_{slag} and T_{water} are the temperature of bulk slag and cooling water, respectively.

$$\lambda = Q \cdot L_{film} / (T_{slag} - T_{water}) \quad (2)$$

Closed porosities of films were calculated using the difference between the apparent densities (ρ_{app}) of films and true densities (ρ_{true}) after being ground into fine powders. The closed porosity can be calculated as $(\rho_{true} - \rho_{app}) / \rho_{true}$. Density was measured using a pycnometer (Ultrapyc 3000, Anton Paar, Graz, Austria). The structures of the solid films on the wide surface of the probe were inspected. The thickness near the center of the films was measured using a point micrometer and the roughness (R_a) of the surface in contacted with the copper probe was measured using a profilometer (Mitutoyo SJ-210, Kawasaki, Japan). The specific measurement positions of thickness and roughness can be found in reference [24]. The surface and internal structures of the slag film were inspected using scanning electron microscopy (SEM, Nova Nanosem 450, FEI Company, Hillsboro, OR, USA) and optical microscopy. Samples for SEM inspection were first mounted in resin and polished using Al₂O₃ suspensions; then, the cross sections of the films were sputter coated using Pt. Crystals in films were identified using X-ray diffraction (XRD, Cu K α , Rigaku Miniflex 600, Tokyo, Japan) after grinding the samples into fine powder. The X-ray diffraction results indicated that the primary crystal in the films was cuspidine (3CaO·2SiO₂·CaF₂, PDF # 00-041-1474). For CaO-SiO₂-CaF₂-based mold fluxes, cuspidine is a dominating crystal phase precipitates in slag films, numerous achievements have been reported on the physical and chemical properties of cuspidine in slag films [25–27].

3. Result and Discussions

3.1. Heat Flux through Slag Film upon Solidification

The graphs of typical heat fluxes through the slag films are shown in Figure 1. The heat flux data indicated that a higher slag bulk temperature resulted in a higher heat flux, which

is in agreement with previous approaches [24]. However, compared with the high-basicity films ($R = 1.28$), the low-basicity films ($R = 0.85$) resulted in heat fluxes with high fluctuation during solidification. Heat flux fluctuation, especially at the initial solidification stage, can deteriorate the cooling uniformity of the microzone on the initial steel shells and cause surface cracks.

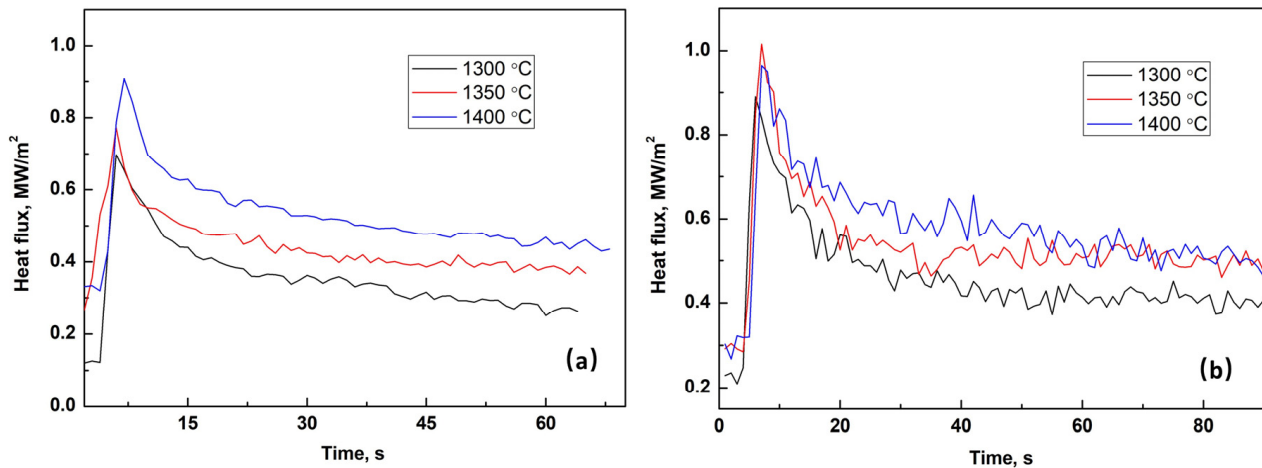


Figure 1. Heat flux through slag films solidified in slag bulk with different temperatures, mold flux with basicity 1.28 (a) and 0.85 (b).

To compare the heat flux fluctuations of the two slags, typical heat flux fluctuation data were obtained, as shown in Figure 2. The mean heat flux value for every three seconds during the film solidification and the corresponding standard deviation were plotted (only the decreasing period of the heat flux curve in Figure 1 was considered). Results indicate that the heat fluxes through the film with higher basicity were more stable upon solidification, especially at the early solidification stage ($t < 20$ s), than through the film with lower basicity. Heat flux fluctuation was caused by the structural evolution of the films upon cooling, which is discussed later.

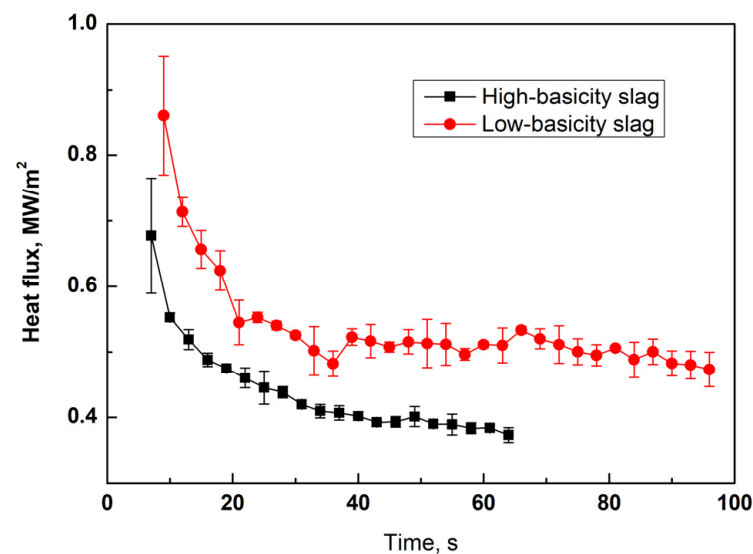


Figure 2. Mean heat fluxes and corresponding standard deviation through slag films during solidification. Bulk slag temperature 1350 °C.

3.2. Structure Evolution of Solid Films

The total thickness of the films, glassy layer thickness of the films, roughness of the film surfaces in contact with the copper wall, and closed porosity of the films were measured.

3.2.1. Total Thickness of Films

Figure 3 shows the total thickness of the films during solidification. Higher slag temperatures and lower basicities resulted in lower film thicknesses and growth velocities. Notably, the thickness non-uniformity of the films became significant at a lower bulk slag temperature (1300 °C). Moreover, the thickness of high-basicity films increased sharply at this temperature, indicating that the internal structures or surface roughness of films changed nonlinearly when slag temperature decreased from 1400 °C to 1300 °C. On the contrary, the decrease in slag temperature had not caused a sharp increase in solidified film thickness for the low-basicity slag. As the temperature fluctuation near meniscus can be intensified in wide slab continuous casting, the sharp increase in film thicknesses at the lower temperature can deteriorate the lubrication capacity of liquid slag films, and which should be the reason that high-basicity mold fluxes usually causes industrial accidents such as sticking or breakouts. The film thickness data indicated that the heat flux fluctuation shown in Figure 1b was not primarily due to film thickness fluctuations but due to the internal structural evolution (including surface roughness) of the films.

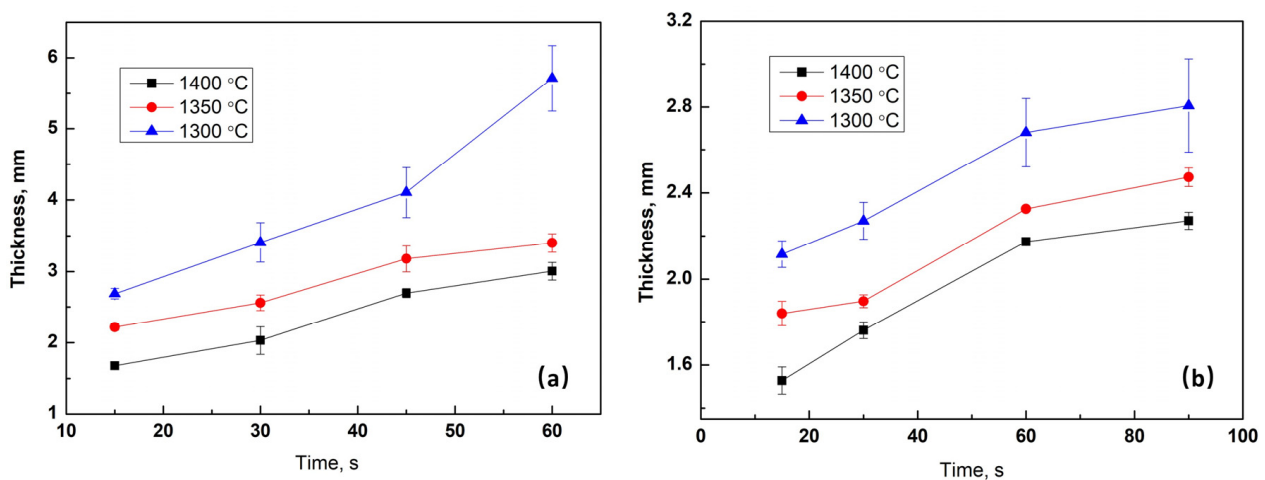


Figure 3. Thickness of films solidified in slag bulk with different temperatures, slag with basicity 1.28 (a) and 0.85 (b) error bars give standard deviations.

3.2.2. Thickness of Glassy Layer of Films

Figure 4 shows the thickness of the film glassy layer after solidification. The reduction velocity of the glassy layer of the high-basicity films was significantly higher than that of the low-basicity films. Because high-basicity slag containing less silico-oxygen complex networks and can provide better kinetic conditions for crystallization. For low-basicity films, an increased bulk slag temperature prevents crystal precipitation. When the slag temperature was 1400 °C, the glassy-layer thickness of the low-basicity film began to decrease until the solidification time exceeded 60 s. When the slag temperatures were 1350 and 1300 °C, the glassy-layer thickness of low-basicity films decreased gradually upon solidification. Figure 5 shows a typical total glassy cross section of a low-basicity film. Closed pores were observed, indicating that pore formation was not directly related to crystallization.

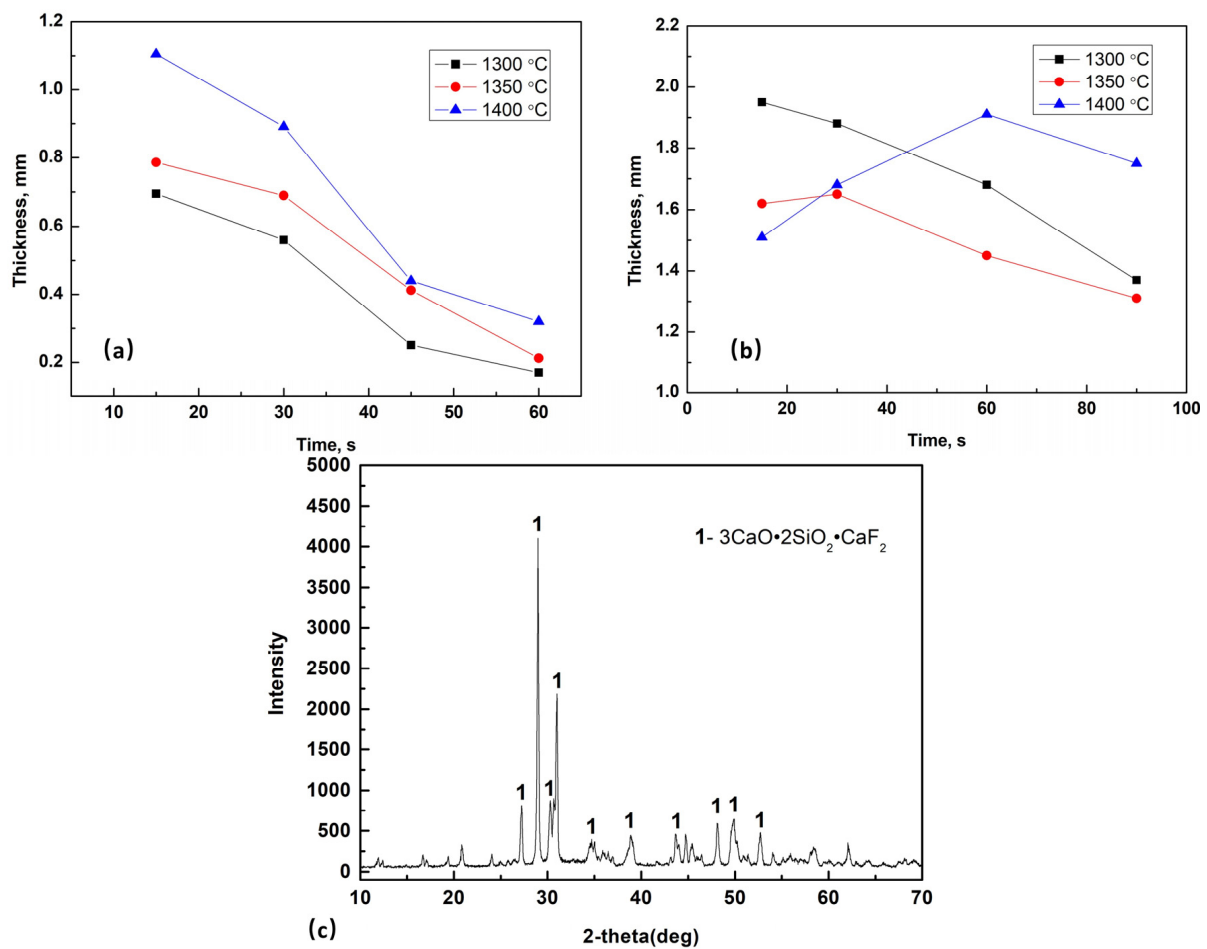


Figure 4. Thickness of glassy layer of films solidified in slag bulk with different temperatures and solidification times, slag with basicity 1.28 (a) and 0.85 (b), and typical XRD pattern of a solidified slag film (c); the film for XRD measurement was obtained in the high-basicity liquid slag bath with 60 s of probe immersion time.

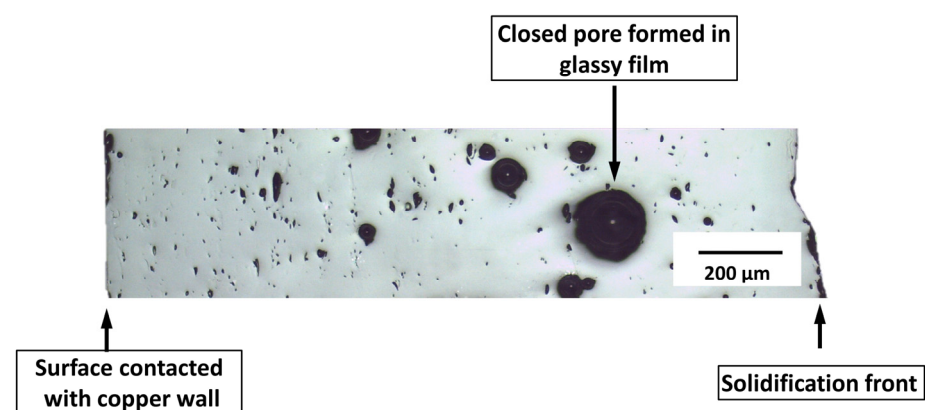


Figure 5. Typical total glassy cross section of a low-basicity film solidified in 1400 °C slag and 30 s solidification time, optical image.

3.2.3. Fusion Cracks within Glassy Layers

As shown in Figures 5 and 6, glass with closed pores and fusion cracks (labeled in Figure 6 using red rectangles) are typical low-basicity films with relatively short solidification times. The irregular morphology of the cracks with fused pore chains indicated that these cracks were not formed after the films left the slag bulk but during solidification.

The formation mechanism of fusion cracks has been discussed in a previous study on low-fluorine mold fluxes [28]. As previously discussed for low-fluorine films, the formation and fusion of cracks within the glassy layer (near the film surface in contact with the copper probes) can lead to high heat flux fluctuation, especially at the initial solidification stage. This is the primary reason for the heat flux fluctuation shown in Figure 1b. However, no obvious fusion cracks were found in the glassy layer of high-basicity films. This is caused by the narrower solidification range that this high-basicity slag has. Industrial applications indicate that compared with CaO-SiO₂-CaF₂-based high-basicity mold fluxes, low-basicity mold fluxes that form glassy films are more likely to cause surface cracks. The large thickness ratio of the glassy layer in the slag films tends to promote the heat flux fluctuation caused by the evolution of fusion cracks. This is one of the reasons that high-basicity mold fluxes with noticeable crystallization tendencies have good performance in preventing slab cracks in continuous-casting peritectic grades.

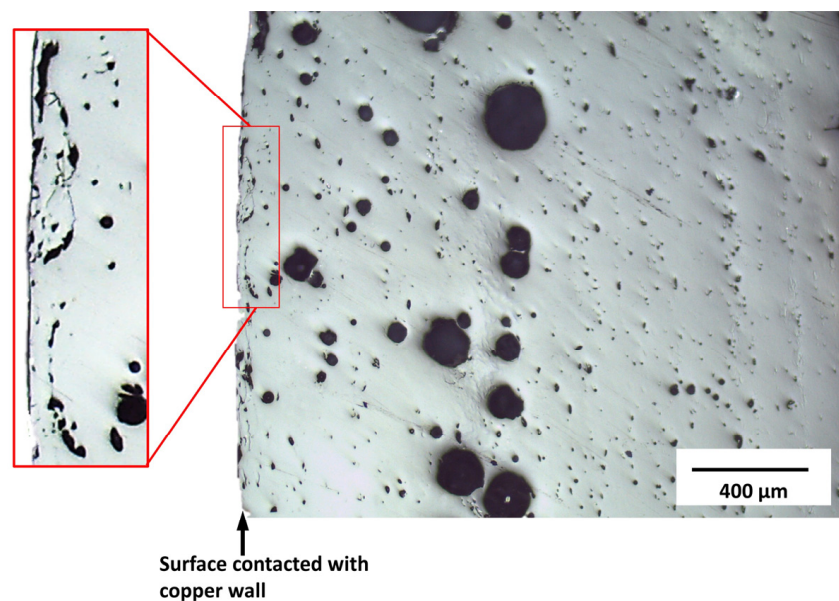


Figure 6. Partial cross section of a low-basicity glassy slag film, bulk slag temperature: 1350 °C, film solidification time: 30 s. Optical image.

3.2.4. Roughness of Film Surfaces Contacted with Copper Wall

The measured roughness R_a of the film surfaces in contacted with the copper probe is shown in Figure 7. Typical morphologies and profile curves of the film surfaces are shown in Figure 8. These results indicate that for high-basicity films, higher slag temperatures result in a higher roughness of the film surfaces in contacted with the copper wall. In this study, low-basicity films presented relatively low surface roughness, and the effect of temperature on the roughness was not noticeable (Figure 7b). Moreover, the surface roughness of the films neither increased with film growth (nor with crystallization). This indicated that the rough surface of the slag films in contacted with the copper wall was formed during the initial stage of solidification and was not caused by crystallization within the films. As the initial steel shells near the meniscus in molds is quite thin and weak, a strong capacity of heat transfer control of initial solidified slag films is required for casting crack-sensitive grades. As the surface roughness of high-basicity films is higher than the low-basicity films have, high-basicity mold fluxes should present better performances on heat flux control and prevention of longitudinal cracks on slabs. This agrees with the commercial performance of high-basicity mold fluxes. Open pores were only detected on surfaces of high-basicity films in this case. This contributed to the high surface roughness and thermal contact resistance of the high-basicity films.

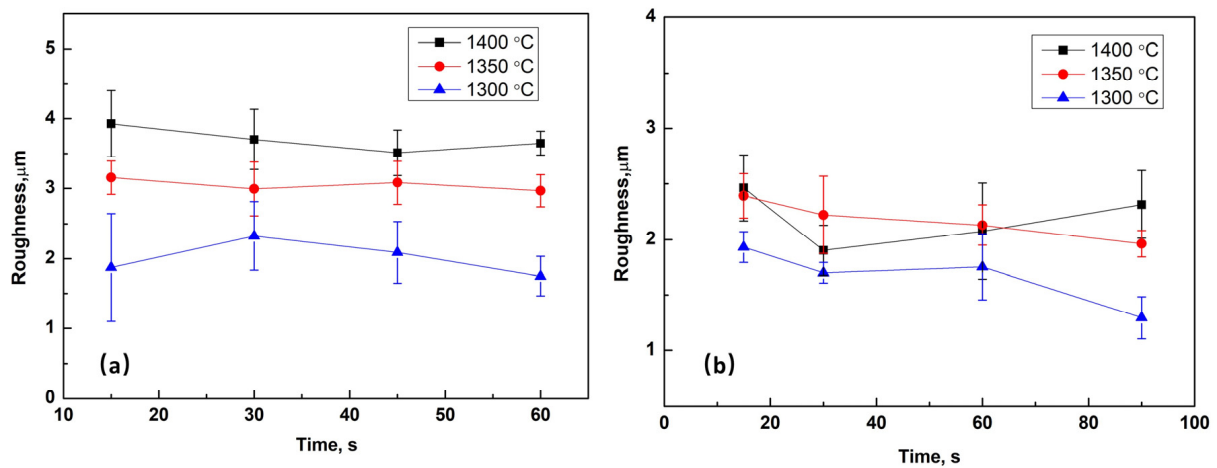


Figure 7. Roughness of film surfaces contacted with copper probe, solidified in slag bulk with different temperatures and solidification times; slag with basicity 1.28 (a) and 0.85 (b).

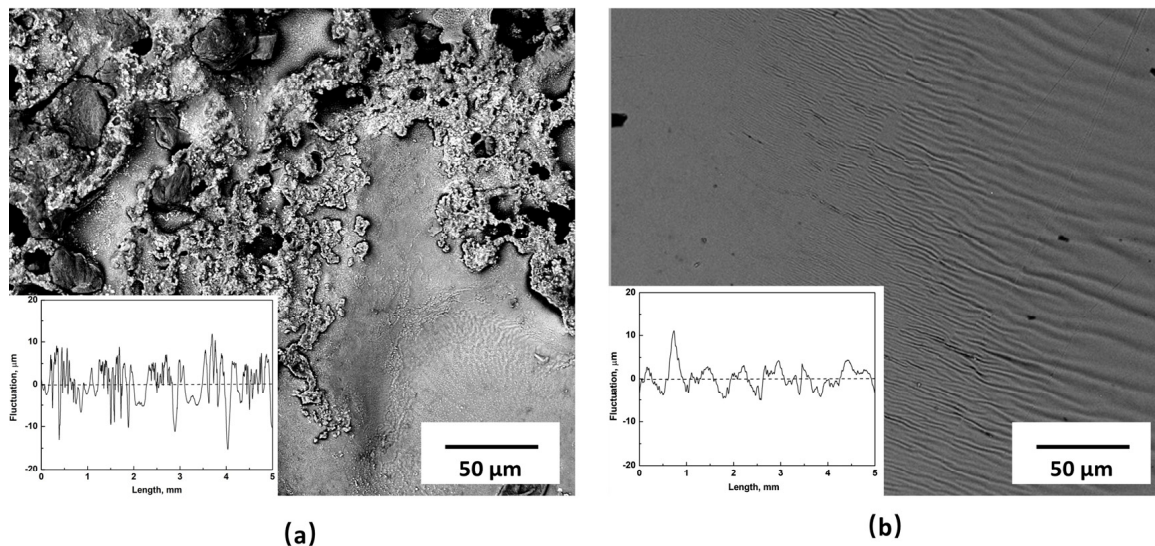


Figure 8. Typical surface and profile curve of a high–basicity film (a) and low–basicity film (b), solidified in 1400 °C slag bulk and 30 s solidification time. Backscattered electron images.

3.2.5. Closed Porosity of Films

Closed pores within the solidified films were analyzed. These pores affected the apparent density and heat transfer behavior of the slag films. In general, the present of closed pore within solidified films can decrease the thermal conductivity of films. Thus, the formation stage of pores upon solidification also should be taken into consideration. Most of these pores were found within the glassy or previous glassy layer (devitrification by precipitating crystals). The measured closed porosity data are presented in Figure 9. For the high-basicity films, most of the pores were formed near the cold side for heat transfer control at the initial solidification stage. This accounts for the decrease in porosity with increasing film thickness. For the low-basicity films, most of the pores precipitated at the center of the film (see Figure 6). This accounts for the increase in the closed porosity of the low-basicity films at the initial solidification stage.

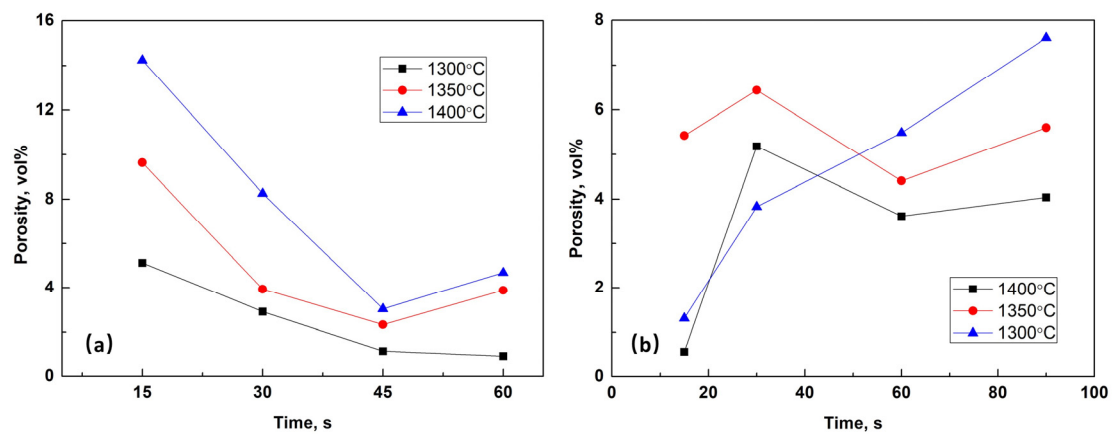


Figure 9. Closed porosity of films solidified in slag bulk with different temperatures and solidification times, slag with basicity 1.28 (a) and 0.85 (b).

3.3. Evolution of Heat Transfer Characteristics of Slag Films upon Solidification

The calculated comprehensive thermal conductivity (including the contact thermal resistance between the slag film and copper wall) under different film solidification times and bulk slag temperatures is shown in Figure 10.

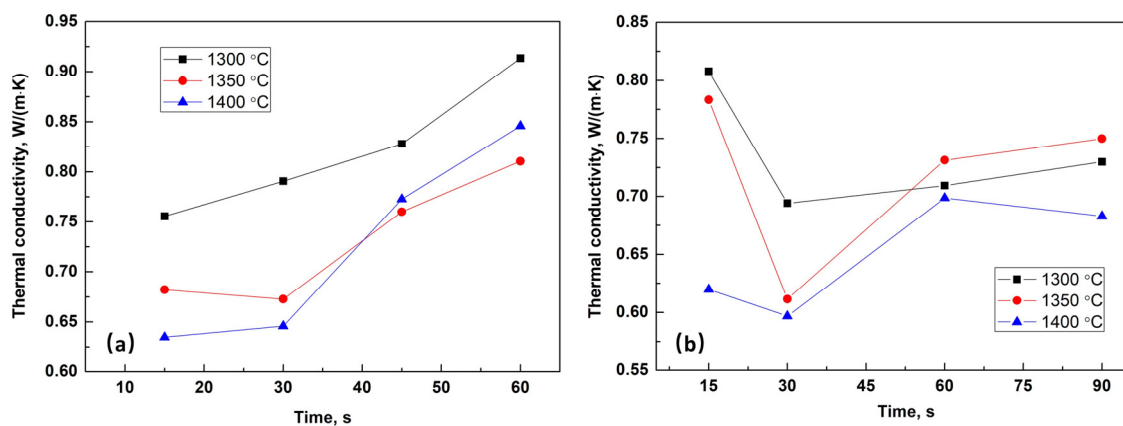


Figure 10. Evolution of thermal conductivities of films upon solidification in molten slag bulk with different temperatures, slag with basicity 1.28 (a) and 0.85 (b).

The results show that at the initial solidification stage (15 s), the high-basicity films have relatively lower comprehensive thermal conductivities, which are mainly attributed to the high surface roughness of the initial films (higher thermal contact resistance between the films and the copper wall), than the low-basicity films have. The high-basicity films exhibit significantly higher heat transfer control capabilities during the initial solidification stage. However, with the rapid increase in film thickness and crystallization (see Figures 3 and 4), the thermal conductivity of the high-basicity films increased significantly. This proves the conclusion of a previous study that, for the same mold flux, crystallized films usually have higher thermal conductivities than glassy films [29]. The thermal conductivity of the low-basicity films first decreased and then increased with the precipitation of crystals within the film. In this case, the comprehensive thermal conductivity of high-basicity films and low-basicity films ranges from 0.63 to 0.91, and 0.62 to 0.81 W/(m·K), respectively.

The structure and comprehensive thermal conductivity evolution of slag films upon solidification have been detected, calculated, and discussed in this study. However, the thermal conductivity value was contributed by all structural factors together. The contribution degree of a single structural factor on heat transfer control upon solidification will be revealed in future work.

4. Conclusions

Two CaO-SiO₂-CaF₂-based commercially used mold fluxes were selected as the basis for this study. The structure and comprehensive thermal conductivity (including the contact thermal resistance between the slag film and copper wall) evolution of the slag films were determined. The results can be summarized as follows:

(1) Compared with the heat flux through the high-basicity slag films, which exhibited high fluctuations through the low-basicity glassy films, especially at the initial solidification stage. This was primarily due to the evolution of fusion cracks within the glass layer near the cold surface of the low-basicity slag films. No obvious fusion cracks were found in the glassy layer of high-basicity slag films.

(2) High-basicity mold fluxes resulted in higher thicknesses, growth velocities, and devitrification velocities of the slag films. The roughness of the surfaces of the high-basicity films in contact with the copper probe was significantly higher than that of the low-basicity films. The rough surface in contact with the copper wall was formed during the early stage of solidification and was not related to crystallization. For high-basicity slag films, higher slag bulk temperature resulted higher surface roughness; the effect of temperature on the roughness was not noticeable for low-basicity mold fluxes.

(3) With the growth and crystallization of the slag films, the comprehensive thermal conductivity of the high-basicity films increased significantly. For the low-basicity films, the thermal conductivities first decreased and then increased after the solidification time exceeded 30 s. The comprehensive thermal conductivity of high-basicity films and low-basicity films ranged from 0.63 to 0.91 and 0.62 to 0.81 W/(m·K), respectively.

The results of this work provide a novel method to reveal the effect of the structural factors of slag films on heat transfer control and to control the heat transfer behavior of slag films upon solidification.

Author Contributions: Conceptualization, X.L. (Xiao Long); methodology, X.L. (Xiao Long), X.L. (Xiang Li) and W.L.; software, S.L. and C.Z.; investigation, X.L. (Xiao Long), X.L. (Xiang Li), H.M., D.L. and C.Z.; data curation, C.Z., H.M. and D.L.; writing—original draft preparation, S.L., H.M. and D.L.; writing—review and editing, X.L. (Xiao Long) and W.L.; and funding acquisition, W.L. and X.L. (Xiang Li). All authors have read and agreed to the published version of the manuscript.

Funding: This research was funded by the National Natural Science Foundation of China (51904083), Natural Science Foundation of Guizhou Province (Qian Ke He Ji Chu [2020]1Y221), Growth Project of Young Scientific and Technological Talents in Universities of Guizhou Province [Qian Jiao He KY Zi (2021)262], and Guizhou Institute of Technology high-level talent research launch project [XJGC20190963].

Data Availability Statement: The data presented in this study are available on request from the corresponding author, upon reasonable request. The data are not publicly available due to privacy.

Conflicts of Interest: The authors declare no conflict of interest.

References

1. Mills, K.C.; Fox, A.B. The role of mould fluxes in continuous casting—so simple and yet so complex. *ISIJ Int.* **2003**, *43*, 1479–1486. [[CrossRef](#)]
2. Mills, K.C. Structure and Properties of slags used in the continuous casting of steel: Part 1 conventional mould powders. *ISIJ Int.* **2016**, *56*, 1–13. [[CrossRef](#)]
3. Wang, W.; Lu, B.; Xiao, D. A review of mold flux development for the casting of high-Al steels. *Metall. Mater. Trans. B* **2016**, *47*, 384–389. [[CrossRef](#)]
4. Cho, J.W.; Emi, T.; Shibata, H.; Suzuki, M. Heat transfer across mold flux film in mold during initial solidification in continuous casting of steel. *ISIJ Int.* **1998**, *38*, 834–842. [[CrossRef](#)]
5. Yoon, D.W.; Cho, J.W.; Kim, S.H. Controlling radiative heat transfer across the mold flux layer by the scattering effect of the borosilicate mold flux system with metallic iron. *Metall. Mater. Trans. B* **2017**, *48*, 1951–1961. [[CrossRef](#)]
6. Bhagurkar, A.G.; Qin, R. The microstructure formation in slag solidification at continuous casting mold. *Metals* **2022**, *12*, 617. [[CrossRef](#)]
7. Mills, K.C. *Treatise on Process Metallurgy*; Elsevier: Oxford, UK, 2014; Volume 3, pp. 435–475.

8. Long, X.; He, S.-P.; Xu, J.-F.; Huo, X.-L.; Wang, Q. Properties of high basicity mold fluxes for peritectic steel slab casting. *J. Iron Steel Res. Int.* **2012**, *19*, 39–45. [[CrossRef](#)]
9. Nakai, K.; Sakashita, T.; Hashio, M.; Kawasaki, M.; Nakajima, K.; Sugitani, Y. Effect of mild cooling in mould upon solidified shell formation of continuous cast slab. *Tetsu-Hagane* **1987**, *73*, 498–504. [[CrossRef](#)]
10. Hunt, A.; Stewart, B. Techniques for controlling heat transfer in the mould-strand gap in order to use fluoride free mould powder for continuous casting of peritectic steel grades. In *Advances in Molten Slags, Fluxes, and Salts, Proceedings of the 10th International Conference on Molten Slags, Fluxes and Salts, Seattle, WA, USA, 22–25 May 2016*; Springer: Cham, Switzerland, 2016; pp. 349–356.
11. Ji, J.; Mao, Y.; Zhang, X.; Chen, W.; Zhang, L.; Wang, Q. Initial solidification and heat transfer at different locations of slab continuous casting mold through 3D coupled model. *Steel Res. Int.* **2021**, *92*, 2000714. [[CrossRef](#)]
12. Yan, X.; Pan, W.; Wang, X.; Zhang, X.; He, S.; Wang, Q. Electrical conductivity, viscosity and structure of CaO–Al₂O₃-based mold slags for continuous casting of high-Al steels. *Metall. Mater. Trans. B* **2021**, *52*, 2526–2535. [[CrossRef](#)]
13. Ji, J.; Cui, Y.; Wang, S.; He, S.; Wang, Q.; Zhang, X. Effect of TiO₂ substituting SiO₂ on the rheological and crystallization behavior of mold slags for casting Ti-containing steel. *Ceram. Int.* **2022**, *48*, 256–265. [[CrossRef](#)]
14. Nakada, H.; Susa, M.; Seko, Y.; Hayashi, M.; Nagata, K. Mechanism of heat transfer reduction by crystallization of mold flux for continuous casting. *ISIJ Int.* **2008**, *48*, 446–453. [[CrossRef](#)]
15. Zhao, H.; Wang, W.; Zhou, L.; Lu, B.; Kang, Y.B. Effects of MnO on crystallization, melting, and heat transfer of CaO–Al₂O₃-based mold flux used for high Al-TRIP steel casting. *Metall. Mater. Trans. B* **2014**, *45*, 1510–1519. [[CrossRef](#)]
16. Susa, M.; Kushimoto, A.; Toyota, H.; Hayashi, M.; Endo, R.; Kobayashi, Y. Effects of both crystallisation and iron oxides on the radiative heat transfer in mould fluxes. *ISIJ Int.* **2009**, *49*, 1722–1729. [[CrossRef](#)]
17. Li, X.; Zhang, Z.; Lv, M.; Fang, M.; Liu, K. Numerical simulation of the fluid flow, heat transfer, and solidification in ultrahigh speed continuous casting billet mold. *Steel Res. Int.* **2022**, *93*, 2100673. [[CrossRef](#)]
18. Yang, J.; Chen, D.; Long, M.; Duan, H. An approach for modelling slag infiltration and heat transfer in continuous casting mold for high Mn–high Al steel. *Metals* **2020**, *10*, 51. [[CrossRef](#)]
19. Wen, G.H.; Zhu, X.B.; Tang, P.; Yang, B.; Yu, X. Influence of raw material type on heat transfer and structure of mould slag. *ISIJ Int.* **2011**, *51*, 1028–1032. [[CrossRef](#)]
20. Xu, C.; Wang, W.; Zhou, L.; Xie, S.; Zhang, C. The effects of Cr₂O₃ on the melting, viscosity, heat transfer, and crystallization behaviors of mold flux used for the casting of Cr-bearing alloy steels. *Metall. Mater. Trans. B* **2015**, *46*, 882–892. [[CrossRef](#)]
21. Anisimov, K.N.; Longinov, A.M.; Gusev, M.P.; Zarubin, S.V. Influence of mold flux on the thermal processes in the mold. *Steel Transl.* **2016**, *46*, 589–594. [[CrossRef](#)]
22. Assis, K.L.S. Heat Transfer through Mold Fluxes: A New Approach to Measure Thermal Properties of Slags. Ph. D. Thesis, Carnegie Mellon University, Pittsburgh, PA, USA, 2016.
23. Assis, K.L.S.; Pistorius, P.C. Improved cold-finger measurement of heat flux through solidified mould flux. *Ironmak. Steelmak.* **2018**, *45*, 502–508. [[CrossRef](#)]
24. Long, X.; He, S.; Wang, Q.; Pistorius, P.C. Structure of solidified films of mold flux for peritectic steel. *Metall. Mater. Trans. B* **2017**, *48*, 1652–1658. [[CrossRef](#)]
25. Masahito, H.; Masayuki, K.; Tadao, W. Influence of Na₂O on phase relation between mold flux composition and cuspidine. *ISIJ Int.* **2004**, *44*, 827–835.
26. Nakada, H.; Fukuyama, H.; Nagata, K. Effect of NaF addition to mold flux on cuspidine primary field. *ISIJ Int.* **2006**, *46*, 1660–1667. [[CrossRef](#)]
27. Watanabe, T.; Fukuyama, H.; Nagata, K. Stability of cuspidine (3CaO·2SiO₂·CaF₂) and phase relations in the CaO–SiO₂–CaF₂ system. *ISIJ Int.* **2002**, *42*, 489–497. [[CrossRef](#)]
28. Zeng, J.; Long, X.; You, X.; Li, M.; Wang, Q.; He, S. Structure of solidified films of CaO–SiO₂–Na₂O based low-fluorine mold flux. *Metals* **2019**, *9*, 93. [[CrossRef](#)]
29. Andersson, S.P.; Eggertson, C. Thermal conductivity of powders used in continuous casting of steel, part 1—glassy and crystalline slags. *Ironmak. Steelmak.* **2015**, *42*, 456–464. [[CrossRef](#)]

Disclaimer/Publisher’s Note: The statements, opinions and data contained in all publications are solely those of the individual author(s) and contributor(s) and not of MDPI and/or the editor(s). MDPI and/or the editor(s) disclaim responsibility for any injury to people or property resulting from any ideas, methods, instructions or products referred to in the content.